Perceptual Issues in Haptic Digital Watermarking

Domenico Prattichizzo, Mauro Barni, Hong Z. Tan, Gloria Menegaz, Alessandro Formaglio

***Abstract*— The growing interest in haptic applications such as skill training, museum displays, multimodal interfaces, aids for people with visual and/or hearing impairments, etc suggests that haptic digital media will soon become widely available, and the need will arise to protect digital haptic data from misuse. One of most common data protection technologies is digital watermarking, which consists of embedding a digital code into multimedia data file. The code should not interfere with the normal use of the media but can be always recovered to prove data ownership. To that end, the embedded code must be imperceptible to the user. Since this requirement also holds for haptic digital media, it is then necessary that human's ability to perceive a hidden signal through a haptic interface be carefully studied. Hence this paper aims at presenting the first results of the psychophysical experiments we have conducted in this context.**

KEYWORDS

Haptics, digital watermarking, perception.

I. Introduction

Haptic interfaces allow physical interactions with virtual 3D objects through the sense of touch. Possible applications include training for minimally-invasive or microscopic surgical procedures, interaction with sculptures such as Michelangelo's *David* that can not be touched directly, perceptualization of multidimensional data sets such as earthquake simulation that can not be easily comprehended through visual displays alone, and assistance to sensory impaired individuals by displaying visual and/or audio information through the haptic sensory channel.

Due to the expected growing importance that digital haptic data will have in the near future, it is easy to predict that the need will soon arise to protect such data from misuse, like unauthorized copying and distribution, or false ownership claims. Among the available technologies to protect digital data, digital watermarking is receiving an increasing attention due to its unique capability of persistently hiding a piece of information within the to-be-protected data [1]. The hidden information can be used to prove ownership, to deny permission of copying the data, to detect tampering, etc. A great deal of research has focused on digital watermarking of audio, images and video while haptic interfaces are inherently related to 3D surfaces.

Despite the fact that 3D models are widely used in several applications such as virtual prototyping, cultural heritage, and entertainment, watermarking of 3D objects is still in its infancy. One of the reasons for this gap lies in the difficulty of extending common signal processing algorithms to 3D data.

The first requirement that any watermarking technique must satisfy is watermark *imperceptibility*. In the case of still images and video sequences, the imperceptibility requirement has triggered a great deal of research about the human visual system, resulting in a number of possible algorithms that exploit the properties of human vision to improve watermark invisibility while keeping the watermark energy constant [15]. First steps in this direction have very recently been taken for the case of 3D watermarking [6]. In this case, the watermark is hosted by the macro-geometry of the surface of the considered virtual object, which is assumed to be represented by a three-dimensional mesh. Accordingly, the intrusiveness of the watermark can be judged in terms of its *visibility* in the rendered version of the mesh. More generally, in applications where the virtual object is sensed through a haptic interface, guaranteeing the imperceptibility of the watermark requires the characterization of the sensitivity of the haptic channel.

Despite an exponential increase in haptics research activities in the last decade, our understanding of how people sense and manipulate objects with their hands is still limited [11]. The most popular haptic interfaces, the PHANToM (SensAble Technologies, www.sensable.com, USA) and the Delta (ForceDimension, www.forcedimension.com, Switzerland), allow us to interact with the virtual environment through one contact point only. Interfaces with higher number of degrees of freedom and with multiple interaction points are available, but are less common or reliable than those with three degrees of freedom and one interaction point.

With the term *haptic rendering*, we refer to a branch of haptics research that deals with the calculation of interaction forces between a virtual representation of the user and a virtual object. In most cases, haptic rendering is a two-step process consisting of shape- and texture-based force rendering. In this context, shape refers to the macro-geometry of an object's surface, as opposed to texture that describes the fine structure, or micro-geometry, of the surface. To render the shape of an object, one can use typical single-point contact rendering algorithms such as the *god-object* [16]. To render the texture of a virtual surface, one can perturb the shape-based force using a texture model [9].

In this paper, we present the results of two psychophysical experiments that investigated the perceptibility and detectability of a hidden signal in the macro- and micro- geometry of the virtual object surface, respectively. In the first experiment, the watermark was embedded into the macro-geometry of the virtual surface by modifying the wireframe of the underlying 3D model. To begin with, a flat surface was chosen so that signals related to the object's shape would not inadvertently mask the detection of the watermark. Nevertheless, the surface

D. Prattichizzo, M Barni, G. Menegaz and A. Formaglio are with the Dipartimento di Ingegneria dell'Informazione of Siena University and H.Z. Tan is with the Haptic Interface Research Laboratory at Purdue University. The corresponding author is Domenico Prattichizzo, Dipartimento di Ingegneria dell'Informazione of Siena University, Email: prattichizzo@dii.unisi.it Phone: +39-0577-234609 Fax: +39-0577-233602.

was represented by a 3D mesh so that this initial work can be readily extended to objects with arbitrary surface shapes. The watermark was modeled as an additive white noise superimposed on the host surface. The goal of the experiment was to estimate the noise intensity threshold as a function of the resolution of the underlying mesh.

The second experiment focused on the micro-geometry of object surfaces by embedding the watermark in the texture data. A simple one-dimensional sinusoidal model was used for both the watermark and the host signal. The goal of this experiment was to investigate whether existing detection threshold data [12], [13], could successfully predict the perceptibility of the watermark. Despite the simplicity of the texture model, this experiment provided the first evidence of the possibility of embedding a haptically imperceptible watermark that can later be detected by means of spectral analysis.

The rest of this paper is organized as follows. Section II presents an overview of the basic principles of watermarking. Sections III and IV describe the macro- and micro-geometry experiments, respectively. Section V concludes and discusses future directions in digital haptic watermarking.

II. Overview of watermarking techniques

Generally speaking any watermarking system can be seen as a communication system consisting of two major components: a watermark embedder, and a watermark detector. The watermark usually consists of a pseudo-random sequence with uniform, binary or Gaussian distribution. It is transmitted through the watermark embedder over the original to-be-marked object (in our case a 3D surface). The watermark detector extracts the watermark from the marked data. Intentional and unintentional attacks and distortions applied to the mesh hosting the watermark further characterize and complicate the transmission channel.

Watermarking techniques can be divided into two main categories: (i) *spatial/temporal domain techniques* that directly add the watermark to pixel values; and (ii) *transformed domain techniques* that add the watermark in the frequency domain.

Once the host features have been chosen, the embedding rule has to be specified. The most common approach to watermark embedding is the *additive* rule according to which $y_i = x_i + \gamma w_i$, where x_i is the i-th component of the original feature vector, w_i the i-th sample of the watermark, γ a parameter controlling the watermark strength, and y_i the i-th component of the watermarked feature vector. Recently a new approach to watermark embedding has been proposed. This approach, commonly referred to as informed watermarking or Quantization Index Modulation (QIM) watermarking [3], can greatly improve the performance of the system as a whole. However, for the sake of simplicity, our analysis focused on additive watermarking, leaving the analysis of QIM schemes for future work.

A crucial role is played by the way the watermark is extracted from data. In *blind* decoding, the decoder does not need the original data (mesh) or any information derived from it in order to recover the watermark. Conversely, *non-blind* decoding refers to a situation where extraction is accomplished with the aid of the original, non-marked data. An important distinction can also be made between algorithms embedding a mark that can be *read* and those inserting a code that can only be *detected*. In the former case, the bits contained in the watermark can be read without knowing them in advance. In the latter case, one can only verify if a given code is present in the document. Though our perceptibility analysis is a general one, we specifically focus on the case of blind watermark detection.

As mentioned in the introduction, an important aspect of any watermarking system is the imperceptibility of the hidden information. For this reason it is of primary importance that the properties of the sensory modality through which the marked object is perceived are carefully studied. In audio watermarking, existing data from studies on the human auditory system have been exploited to better hide the watermarking signal within the host audio. More relevant to the 3D scenario is the case of still image watermarking. Several models of the human visual system have been modified and exploited to ensure the invisibility of the hidden signal. In most cases Watson's simple model of vision has been adopted [5] leading to watermarking systems working in the DCT (discrete cosine transform) or DFT (discrete Fourier transform) domain. Watson's model is able to predict the visibility of a sinusoidal grating (watermarking signal) superimposed on another sinusoidal grating (host signal). One problem with visual watermarking in the frequency domain is the lack of spatial localization, hence alternative models operating in the wavelet domain have been proposed that have led to improved watermark invisibility. As far as 3D meshes are concerned, few studies have been published so far. Of those studies, two different approaches have been taken: judging the visibility of the watermark in some selected views of the rendered mesh, and allowing the observer to freely play with the mesh, e.g., by zooming and rotation [6]. Much more work is needed before watermark visibility in 3D objects can be fully understood. To the best of our knowledge, no previous work on *haptic* watermark perceptibility has been presented with the exception of the studies carried out by the authors of the present paper.

For a more detailed discussion of watermarking issues, readers are referred to [2], [5].

III. Experiment I: macro-geometry watermarking

The first experiment was aimed at estimating the perceptibility threshold of a watermark modeled as a white noise with uniform distribution embedded in the macro-geometry description of the surface. The simplest case of a flat surface implicitly described by a 3D mesh was considered. The same representation was used for both the host plane and the watermark. The 3D meshes were encoded in data structures representing the spatial coordinates of all the vertices as well as their interconnections. A virtual mesh was haptically displayed by a force feedback device that allowed single-point contact mediated by a stylus, as depicted in Fig.1. The information about the surface shape was conveyed via the direction of the reaction forces that corresponded to the

Fig. 1. A subject touching a virtual surface through a stylus-like device.

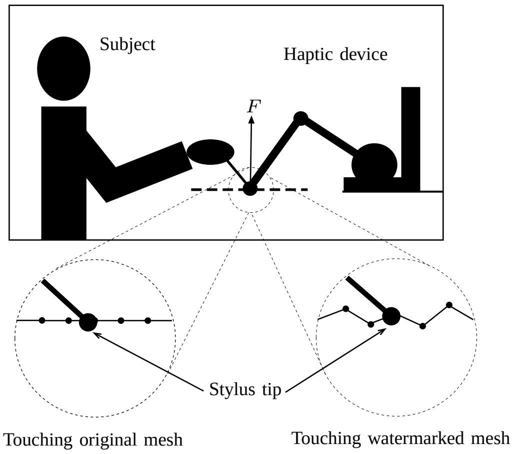

Fig. 2. Experimental set-up. Bottom left: host mesh; Bottom right: watermarked mesh.

normal vectors to the mesh. The force interaction model did not include friction.

The digital watermark can be embedded in the macro-geometry of the surface by modifying the data matrices according to the additive rule. In this case, the watermark signal was added to the height of the corresponding vertex of the mesh. The *strength* of the watermark was represented by the noise spectral power of the equivalent noise model. Human sensitivity to the noise was estimated as the minimum noise level required for the watermark to become detectable. Since the resolution of the mesh, i.e. the dimension of triangle elements, may vary with application specifications and surface shapes, the experiment was conducted using several 3D meshes with different resolution. This way, the relationship between the sensitivity to the watermark strength and the size of the triangular mesh elements could be established.

A. Methods

The host surface was a horizontal square plane of size $15 \times 15cm^2$ represented by a 3D triangular mesh and placed in front of the subject. Let $\mathbf{v}(i)$ be the 3D vector of the i-th triangle vertex and $\mathbf{n}(i)$ the surface normal defined at this point. As mentioned earlier, the embedded watermark altered the mesh vertices according to the following rule:

$$\mathbf{v}_w(i) = \mathbf{v}(i) + w(i)\mathbf{n}(i),$$

where $\mathbf{v}_w(i)$ was the i^{th} watermarked vertex and $w(i)$ the watermark noise model. Specifically, a uniform distribution was assumed for $w(i)$ in the range $\{-\Delta, +\Delta\}$. The corresponding frequency domain representation of the watermark noise consisted of a constant spectral power over all frequencies, $P_w(\omega) = \Delta^2/12$.

The human subjects explored the virtual surfaces using a PHANToM force-feedback device (model Desktop, SensAble Technologies, Inc., Woburn, MA, USA). They held the stylus of the PHANToM with their right hand and stroked the surface, as illustrated in Fig. 2.

An impedance model [16] was used to render a force F to the subject's hand (Fig.2) when the stylus tip was inside the virtual surface. No force was displayed when the stylus was outside the virtual surface.

A two-interval forced choice (2IFC) three-down one-up adaptive procedure was used to estimate the watermark detection threshold [7]. According to the 2IFC paradigm, there were two stimulus alternatives, one with the host mesh, and the other with the watermarked mesh. On each trial, the two surfaces were presented to the subject in random order. The subject's task was to report which surface (the first or the second) contained the plane with the watermark. As is typical of most adaptive procedures, no trial-by-trial correct-answer feedback was provided during the experiment. According to the three-down one-up adaptive rule, the watermark strength was decreased after three consecutive correct answers and increased after a single wrong answer, as follows:

$$\begin{cases} \Delta(0) & = & 2mm & \\ \Delta(i+i) & = & 0.5\Delta(i) & \text{(after 3 correct responses)} \\ \Delta(i+i) & = & 1.5\Delta(i) & \text{(after 1 incorrect response)} \end{cases}$$

where the initial value $\Delta(0) = 2$mm was found to be clearly perceivable in a pilot test.

The stop condition was reached after 6 reversals. A *reversal* occured when the watermark strength changed from increasing to decreasing, or vice versa. It now follows that the total number of trials per run was not fixed *a-priori*, but was determined adaptively to meet the stop condition described above. A sketch of a typical staircase sequence produced during one experimental run is given in Figure 3. The detection threshold was computed by taking the average of the peaks and valleys over the 6 reversals within one staircase sequence.

The experiments were arranged in two blocks per subject: a practice block and an experimental block. Each block consisted of seven runs corresponding to the seven sizes of the side of the triangular mesh elements ranging from 2 to 10mm. The estimated detection thresholds from the second block were recorded for each subject as a function of mesh resolution. Five subjects, aged between 22 and 25, participated in the experiment. All were right-handed with no known sensorimotor impairments. Their prior experience with the PHANToM device varied from naïve to expert.

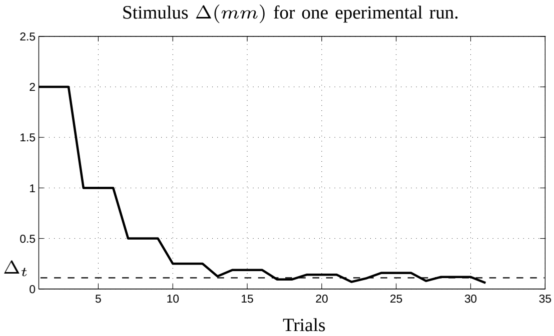

Fig. 3. A typical staircase sequence for one experimental run. In this case, the triangle side length was $l = 2.85mm$. The watermark strength was determined by the parameter Δ. The dashed line represents the estimated detection threshold.

B. Results and discussion

The mean and standard deviation of the estimated detection thresholds in terms of the watermarking strength Δ were calculated from the data of all the subjects. They are shown in Figure 4 as a function of the triangle side length l. Note that the procedure we followed was a within-subject design meaning that each subject was tested with all values of the triangle mesh side length. As a result, the effect of side length on watermark detection threshold could be assessed within each subject. Due to the relatively small number of subjects tested and their different level of prior experience with haptic interfaces, some between-subject variability in thresholds were expected, thereby explaining relatively large standard deviations in the plot of Fig.4.

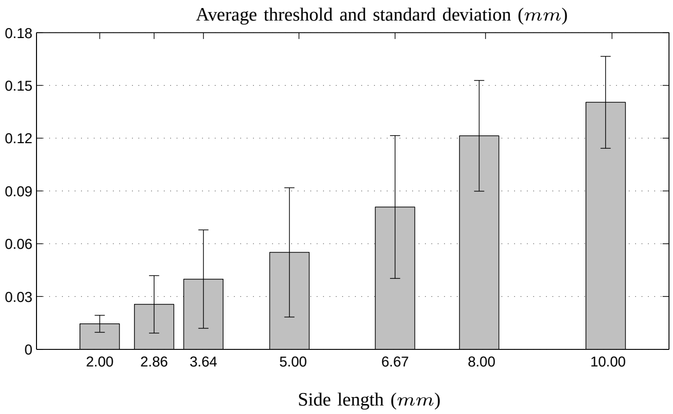

Fig. 4. Average thresholds over triangle side length.

In general, watermark detection threshold increased as a function of the mesh resolution, indicating that more noise can be embedded in surfaces with coarser representation. The values of the thresholds can be used to adjust the strength of the watermark signal as a function of the local geometrical features of the host surface so that imperceptibility can be guaranteed.

IV. Experiment II: micro-geometry watermarking

The second experiment considered the watermarking of haptic virtual texture, i.e. the micro-geometry of surfaces [10]. While the first experiment aimed at estimating the sensitivity to watermark as a function of the size of the triangular mesh of the macro-geometry, the goal of the second experiment was to investigate the exploitability of existing data in the literature for predicting the perceptibility of watermarks embedded in the micro-geometry. Past research on human detection thresholds for sinusoidal stimuli [12], [13] has established the minimum signal strength required for producing a sensation. Since we chose to model haptic virtual textures (both the host and the watermark signals) using sinusoidal gratings, it was anticipated that the perceptibility of watermarks could be predicted using existing detection thresholds.

When a virtual flat haptic surface with a superimposed sinusoidal grating (texture) is explored with a force-feedback device such as the PHANToM, texture information is conveyed through vibration. Previous work has shown that the temporal signal contributing to texture perception is characterized by a spectral peak of the force or position signals recorded near or at the stylus tip [4]. The frequency of this peak is determined by the spatial period of the sinusoidal grating and the speed at which the textured surface is stroked. The amplitude of the peak determines the perceived intensity (or roughness) of the texture.

It now follows that digital watermarking of virtual haptic texture can be considered in the spectral domain: given a host texture signal, an additional spectral peak at a different frequency with an amplitude below human detection threshold (the watermark) can be added that guarantees its imperceptibility. Therefore, the second experiment employed a simplified version of the additive watermarking method outlined earlier.

A. Methods

The height map of the host texture signal was defined by

$$h(x) = A_h \sin\left(\frac{2\pi}{L_h}x\right) + A_h$$

where A_h = 1 mm and L_h = 2 mm. The symbols A and L denoted the amplitude and the spatial wavelength of the sinusoidal gratings, respectively. The watermarked texture signal was defined by

$$h(x) = A_h \sin\left(\frac{2\pi}{L_h}x\right) + A_h + A_w \sin\left(\frac{2\pi}{L_w}x\right) + A_w$$

where L_w = 5 mm, and A_w was either 0.2 (condition 1) or 0.5 mm (condition 2). Figure 5 illustrates the one-dimensional sinusoidal texture model. As in the first experiment, the feedback force F in Figure 5 was computed according to the impedance model [16].

In the spatial domain, the watermarked texture signal was a modulated sinusoidal signal (Figure 6, bottom trace). In the frequency domain, it exhibited two spectral peaks (Fig. 7). The upper panel in Figure 7 shows the spectral density of $p_z(t)$ (solid line) for condition 1 where the weaker watermark signal was embedded in the host texture signal. The $p_z(t)$ data were recorded from a single stroke of the watermarked textured surface using the PHANToM haptic device. The dashed line in the same panel shows the human detection thresholds taken from the literature [12]. The two spectral

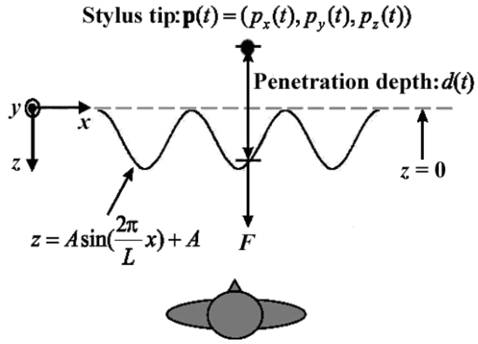

Fig. 5. Bird's-eye view of subject, textured vertical plane, and coordinate frame. The dashed line indicates the flat vertical plane upon which a one-dimensional sinusoidal texture model was superimposed. Subjects stroked the textured surface along the x-axis. Penetration depth was measured as the distance between the stylus tip and the point on the textured surface along the z-axis.

peaks corresponded to the watermark ($\approx$ 40 Hz) and host ($\approx$ 76 Hz) signals, respectively. The lower panel in Fig. 7 shows the same for condition 2 where the stronger watermark signal was used. The perceptibility of the two watermarks could be predicted by comparing the watermark peaks with the corresponding human detection thresholds. Since the peak for the weaker watermark was at roughly the same level as the human detection threshold, we did not expect the subjects to be able to detect it. The peak for the stronger watermark, however, was clearly above the human detection threshold. We therefore expected this watermark to be easily perceived by our subjects.

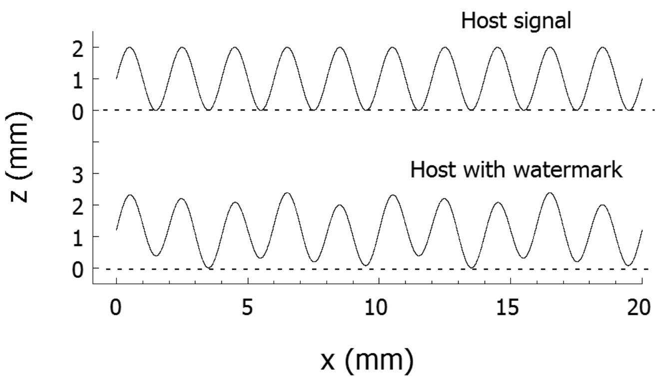

Fig. 6. Spatial representation of stimuli. Top trace shows the z vs. x sinusoidal grating for the host texture alone ($A_h = 1$ mm, $L_h = 2$ mm). Bottom trace shows the same host signal with an embedded watermark ($A_w = 0.2$ mm, $L_w = 5$ mm).

A one-interval two-alternatives forced-choice paradigm was used to measure the subject's ability to discriminate the host texture from the watermarked texture. On each trial, the subject felt either the host texture alone, or the host texture with the watermark. Their task was to respond "1" to the host texture and "2" to the watermarked host texture. No trial-by-trial correct-answer feedback was provided during data collection. Each subject performed four 100-trial blocked runs, two for

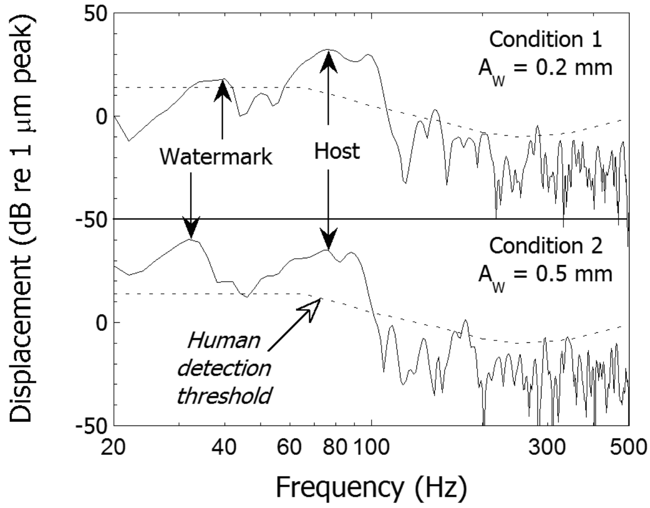

Fig. 7. Power spectral densities of $p_z(t)$ for the two watermarked textures (solid lines) and human detection thresholds (dashed lines). The upper and bottom panels correspond to the weaker and stronger watermarks, respectively. The locations of the spectral peaks corresponding to the watermark and the host textures are indicated by arrows.

condition 1 and two for condition 2. The order of the four runs was randomized for each subject. At the beginning of each run, subjects familiarized themselves with the stimuli by entering either 1 or 2 on a keyboard to feel the corresponding texture. Training was terminated by the subjects whenever they were ready.

Data from each condition formed a 2×2 stimulus-response matrix consisting of 200 trials. Instead of calculating the percent-correct scores which are often confounded by subjects' response biases, we estimated the sensitivity index d' that provided a bias-free measure of the discriminability between the host and watermarked host textures (i.e., the perceptibility of the watermark signal) [8][14]. A d' value of 0.0, 1.0 or 2.0 corresponds to a percent-correct score of 50%, 69% or 84%, respectively, assuming no response biases.

Five subjects, aged 25-39, participated in the experiment. All were right-handed with no known sensorimotor impairment with their hands. Their prior experience with the PHANToM device varied from naïve to expert.

B. Results and discussion

Shown in Fig. 8 are the values of *sensitivity index* d' for five subjects. The d' values were essentially 0 in condition 1 where the weaker watermark signal was used, indicating that the subjects could not tell the difference between the host texture alone and the watermarked texture. In condition 2 where the stronger watermark signal was used, the values of d' were in the range 1.39 - 2.63 indicating high discriminability. Therefore, the stronger watermark signal was clearly perceivable to all the subjects.

The spectral-domain analysis of the texture signals provides a means for detecting watermarks embedded in a texture signal. The frequency of the host or the watermark texture signal is around $|v|/L$ where v is the average stroking velocity

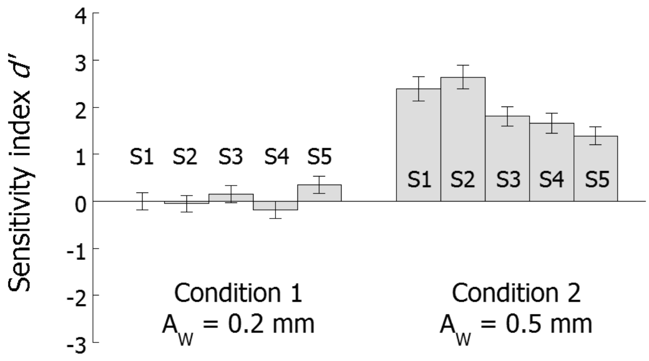

Fig. 8. Experimental results. Shown are the sensitivity indices and the corresponding standard deviations for subjects S1-S5 under the two watermarking conditions.

and L the spatial period of the sinusoidal grating [4]. The average stroking velocity can be estimated from the position data along the lateral stroking direction [$p_x(t)$ in Figure 5]. One can then look for a spectral peak near $|v|/L_w$ to detect the watermark.

V. Conclusions and future perspectives

We have taken a first step towards the analysis of the haptic perceptibility of digital watermarks. Two psychophysical experiments were conducted with the aim to measure the human ability to haptically perceive the presence of a small signal hidden in a host virtual surface. We separately investigated the perceptibility and detectability of a hidden signal in the macro- and micro-geometry of the virtual object, i.e. a signal embedded into a 3D mesh and into textural data, respectively.

As it is the case for any novel inter-disciplinary research framework, many issues are left open for further investigation. Among the many aspects that deserve investigation are the generalization to more complex shapes, the use of different models for the watermarking signal, as well as the perceptual impact of different rendering techniques.

Moreover, we are planning to compare haptic and visual perceptibility using the same object and surface representations, in order to analyze whether the constraints set by the haptic channel are more or less stringent than those set by the visual channel, and if these constraints follow the same rules in both domains. To avoid reinventing the wheel, we will systematically test the perceptibility of common visual watermarking techniques in haptically rendered 3D objects at both macro- and micro-geometry levels, and compare the perceptibility thresholds for the visual and haptic sensory modalities. To the extent that some of the existing watermarking techniques can be readily applied to the haptics domain and possibly result in higher thresholds (i.e., harder to perceive) by the sense of touch, we will have found new ways to achieve multimodal imperceptibility by employing existing visual watermarking algorithms. It is also quite possible that lower detection thresholds may be found using multimodal (visual and/or haptic) interfaces, in which case new watermarking techniques need to be developed. The characterization of the two sensory modalities under both unimodal (haptic or visual stimulation alone) and bimodal (visuo-haptic stimulation) conditions will allow us to determine which sensory modality and/or stimulation condition ultimately sets the boundary for the detectability of haptic/visual watermarks. We envision that with the availability of lower-cost commercially-available haptic interfaces, the area of haptic and multimodal digital watermarking will soon become the next fruitful territory for research on digital watermarking.

VI. Acknowledgements

This work was supported in part by Fondazione Monte dei Paschi di Siena and by Università di Siena under Grant PAR-2003 and PRIN-2006 AIDA, and by US National Science Foundation awards under Grant 0098443-IIS and 0328984-CCF.

References

[1] M. Barni and F. Bartolini. Data hiding for fighting piracy. *Signal Processing Magazine*, 21(2):28–39, March 2004.

[2] M. Barni and F. Bartolini. *Watermarking Systems Engineering: Enabling Digital Assets Security and Other Applications*. Marcel Dekker, 2004.

[3] B. Chen and G. Wornell. Quantization index modulation: a class of provably good methods for digital watermarking and information embedding. *IEEE Trans. on Information Theory*, 47(4):1423–1443, May 2001.

[4] S. Choi and H.Z. Tan. Perceived instability of virtual haptic texture. i. experimental studies. *Presence: Teleoperators and Virtual Environments*, 13:395–415, 2004.

[5] I. J. Cox, M. L. Miller, and J. A. Bloom. *Digital Watermarking*. Morgan Kaufmann, 2001.

[6] M. Corsini M. Barni E. Drelie Gelasca, T. Ebrahimi. Objective evaluation of the perceptual quality of 3d watermarking. In *Proc. of ICIP 2005, IEEE International Conference on Image Processing*.

[7] H. Levitt. Transformed up-down methods in psychoacoustics. *The Journal of the Acoustical Society of America*, 1970.

[8] N. A. Macmillan and C. D. Creelman. *Detection Theory: A User's Guide*. New York: Lawrence Erlbaum Associates, 2nd edition, 2004.

[9] T.H. Massie. Initial haptic explorations with the Phantom: Virtual touch through point interaction. Master thesis, MIT, 1996.

[10] D. Prattichizzo, M. Barni, H. Z. Tan, and S. Choi. Perceptibility of haptic digitalwatermarking of virtual textures. In *Proc. World Haptics Conference*, pages 50–55, Pisa, Italy, March 18-20 2005.

[11] J.K. Salisbury. Making graphics physically tangible. *Communications of the ACM*, 42(n), Aug. 1999.

[12] R. T. Verrillo. Effect of contactor area on the vibrotactile threshold. *J. Acous. Soc. Am.*, 35:1962–1966, 1963.

[13] J. M. Weisenberger and M. J. Krier. Haptic perception of simulated surface textures via vibratory and force feedback displays. In *Proc. of the ASME Dynamic Systems and Control Division*, pages 55–60, 1997.

[14] T.D. Wickens. *Elementary Signal Detection Theory*. Oxford University Press, New York, USA, 2002.

[15] R. B. Wolfgang, C. I. Podilchuk, and E. J. Delp. Perceptual watermarks for digital images and video. *Proceedings of the IEEE*, 87(7):1108–1126, July 1999.

[16] C. Zilles and K. Salisbury. A constraint-based god-object method for haptic display. In *Proc. IEEE/RSJ Int. Symp. Intelligent Robots and Systems*, volume 3, 1995.